PCCP

RSC Publishing

PAPER

View Article Online
View Journal | View Issue

Stability and physical properties of a tri-ring based porous g-C_4N_3 sheet

Cite this: *Phys. Chem. Chem. Phys.*, 2013, **15**, 7142

Xiaowei Li, Shunhong Zhang and Qian Wang*

Received 23rd December 2012,
Accepted 14th March 2013

DOI: 10.1039/c3cp44660c

www.rsc.org/pccp

Due to their porosity and biocompatibility, C–N based graphitic sheets are currently attracting much attention. Here we present our findings on a new structure of a g-C_4N_3 sheet composed of the tri-ring heptazine-like units, which is energetically more stable, more elastic and isotropic than the previously proposed structure consisting of the single-ring triazines. Dynamics and thermal stability of the new structure are confirmed using phonon spectrum calculations and molecular dynamics simulations. Based on hybrid density functional theory, we demonstrate that the tri-ring unit based g-C_4N_3 is a semiconductor with a small band gap, sharp optical absorption peaks and high absorption intensity. Although the new structure is nonmagnetic, ferromagnetism can be introduced and the optical absorption can be tuned by applying a small strain.

Inspired by the unique properties of graphene, increasing attention is currently paid to graphitic C–N sheets. Among them, g-C_3N_4 has potential applications in fuel cells, photocatalysis, and hydrogen production,[1–8] and g-C_4N_3 displays ferromagnetism[9] originating from s and p electrons. Thus, in the application of spintronics, it has advantages over most of the studied spintronic materials, such as transition metal (TM) impurities doped GaN and ZnO where magnetism is due to d electrons.[10] Since s and p electrons have weaker spin–orbit coupling and smaller hyperfine interaction as compared to d electrons, consequently, they have a longer spin coherence time, which is required for an ideal spintronic material. In addition, C–N based materials are more biocompatible than pure carbon.[11,12] So C–N based magnetic sheets are very promising for the applications in spintronics as well as in biotechnology. However, a systematic study on the stability, electronic structure, optical properties and magnetism of C–N based materials is still lacking. Previous studies found that g-C_3N_4 has several structural isomers which can be categorized into two families based on their distinct heterocyclic building blocks: single-ring triazine or tri-ring heptazine,[13] exhibiting different electronic and magnetic properties, and accordingly having different potential applications. In a recent study of g-C_4N_3,[9] the authors only considered the structure composed of the single-ring triazines (labeled g-s-C_4N_3 hereafter), which was found to be ferromagnetic (FM). Thus, the following questions arise: can one construct a new structural model of g-C_4N_3 composed of the tri-ring units (labeled g-t-C_4N_3)? Is this new structure energetically and dynamically stable? Is it still FM like the reported g-s-C_4N_3? What novel physical properties would this new structure have and how to tailor them for potential applications? In this paper, we answer these questions based on a systematic density functional study.

First-principles calculations on g-C_4N_3 sheets are performed using spin-polarized density functional theory (DFT) as implemented in Vienna *ab initio* Simulation Package (VASP code).[14] Exchange–correlation functional is treated by the Perdew–Burke–Ernzerhof (PBE) form within the generalized gradient approximation (GGA) scheme.[15] The electron–ion interaction is described by projector-augmented-wave (PAW) potentials. The energy cutoff, convergence criteria for energy and force are set to 520 eV, 0.01 meV and 0.001 eV $Å^{-1}$, respectively. The Brillouin zones are represented by Monkhorst–Pack special *k*-point meshes of $n \times n \times 1$, where $n = 7$ for the calculations of geometry relaxation, and $n = 15$ for the density of states (DOS) and the optical properties, respectively. The vacuum space in the non-periodic direction is not less than 15 Å, which is enough to avoid the interaction between the two neighboring images.

The phonon spectrum is calculated using the finite displacement method, as implemented in the Phonopy code.[16] For the calculations of the elastic tensor, six finite distortions of the lattice are used to derive the elastic constants from the strain–stress relationship.[17] The ionic contributions are determined by inverting the ionic Hessian matrix and multiplying with the internal strain tensor.[18] To calculate the optical properties, the imaginary part of dielectric function is determined by a summation over empty states in the whole Brillouin zone.[19] In order to

Center for Applied Physics and Technology, College of Engineering, Peking University, Beijing 100871, China. E-mail: qianwang2@pku.edu.cn

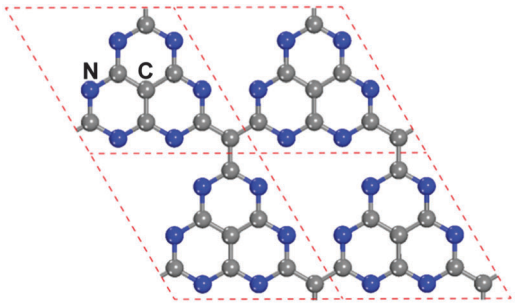

Fig. 1 Fully relaxed structure of the g-t-C_4N_3 sheet composed of the tri-rings. The unit cell is marked by a dashed rhombus.

determine the ground state of g-t-C_4N_3 when applying different tensile strains, a supercell consisting of 2 × 2 unit cells is used to study the magnetic coupling between the two nearest unit cells. The energy difference ΔE between the FM and antiferromagnetic (AFM) or nonmagnetic (NM) states is defined as $\Delta E = E_{AFM(NM)} - E_{FM}$.

The g-t-C_4N_3 sheet consists of tri-ring heterocyclic units and sp^2 hybridized C atoms, as shown in Fig. 1. The lattice constant is 7.17 Å which is larger than that of the g-C_3N_4 (7.08 Å)[20] due to the existence of C–C bonds. It is found that all atoms are not strictly in a plane. The edge N atoms shift upward or downward from the basal plane by about 0.1 Å alternately. In order to study the energetics, we calculated the total energy for the two structures of g-s-C_4N_3 and g-t-C_4N_3, and found that the former one is higher in energy than the latter one by 0.043 eV per atom, indicating that the g-t-C_4N_3 is energetically more stable than the g-s-C_4N_3. Meanwhile, we note that the shift (0.3 Å) of the edge N atoms from the basal plane in g-s-C_4N_3 is larger than that (0.1 Å) of the g-t-C_4N_3. Our calculated structural distortion of g-s-C_4N_3 is in good agreement with a previous study.[9]

In order to study the dynamic stability of the g-t-C_4N_3 structure, the 4 × 4 supercell is used to reduce the constraint of the lattice. First-principles molecular dynamics simulations are performed at room temperature (300 K) with a time step of 1 fs. The fluctuations in total energy and temperature with time steps are shown in Fig. 2. After 5000 steps, the framework is still intact. The phonon spectrum and phonon frequency density of state are further calculated and plotted in Fig. 3. No imaginary phonon mode is found in the whole Brillouin zone. This confirmed the dynamic stability of the tri-ring based g-t-C_4N_3 structure.

The distinct geometry of the two g-C_4N_3 may imply different physical properties. We first focus on their mechanical properties. To test our method, we begin with graphene sheets. The calculated elastic constants are $C_{11} = C_{22} = 339$ GPa nm, $C_{12} = C_{21} = 74$ GPa nm, and $C_{66} = 132$ GPa nm, respectively, which agree well with the results of experiment[21] and *ab initio* calculations.[22] For the new g-t-C_4N_3 structure, its elastic constants are calculated to be $C_{11} = C_{22} = 148$ GPa nm, $C_{12} = C_{21} = 54$ GPa nm, and $C_{66} = 47$ GPa nm. Therefore, it is mechanically isotropic. Differently, the g-s-C_4N_3 sheet is found to be anisotropic, and the corresponding elastic constants are calculated to be $C_{11} = 165$ GPa nm, $C_{22} = 155$ GPa nm, $C_{12} = C_{21} = 56$ GPa nm, and $C_{66} = 63$ GPa nm, respectively, which are slightly larger

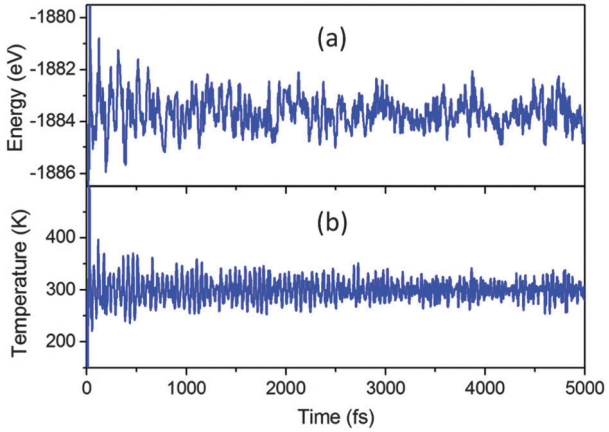

Fig. 2 (a) Total energy and (b) temperature fluctuations with respect to MD steps at 300 K for the g-t-C_4N_3.

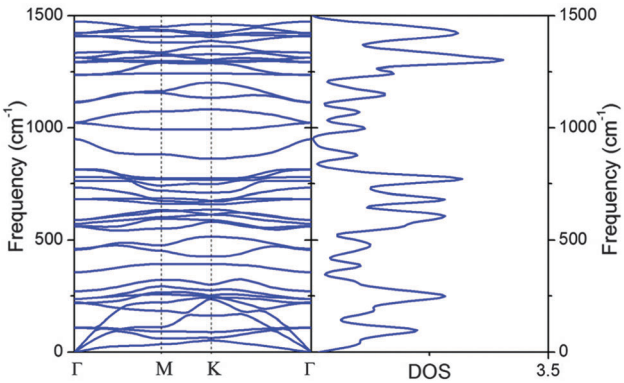

Fig. 3 Calculated phonon spectrum (left) and frequency DOS (right) for the g-t-C_4N_3. For the phonon dispersion band, the high symmetric path in the Brillouin Zone is: $\Gamma(0, 0, 0) \rightarrow M(1/2, 0, 0) \rightarrow K(1/3, 1/3, 0) \rightarrow \Gamma(0, 0, 0)$.

than those of the new g-t-C_4N_3 structure. The underlying reason is that the new structure has larger pores. Therefore, we see that the tri-ring based structure becomes more elastic and isotropic in mechanical properties, namely the new structure can be stretched more easily when applying a tensile strain. Therefore, in the following, the electronic, magnetic, and optical properties of g-t-C_4N_3 with a tensile strain from 0.0% to 5.0% are studied. We define the biaxial tensile strain as $(L–L_0)/L_0$*100%, where L_0 ($L_1 = L_2 = L_0$) and L are the lattice constants of g-C_4N_3 in equilibrium and in strained states, respectively.

The free g-t-C_4N_3 sheet is found to be a NM semiconductor with a smaller band gap of 0.3 eV. The band structure and partial DOS (PDOS) are plotted in Fig. 4(a) and (b). There are some flat energy bands near the Fermi level. The valence band maximum (VBM) is mainly contributed by the p_z orbital of the C atoms and p_x, p_y, p_z orbitals of the N atoms, while the conduction band minimum (CBM) is dominated by p_x and p_y orbitals of the N atoms. The partial charge densities of VBM and CBM at Γ and M *k*-points, respectively, demonstrate that the two bands near the Fermi level are mainly occupied by p orbitals of both A sites (N and C atoms) if defining N atoms at the edges as

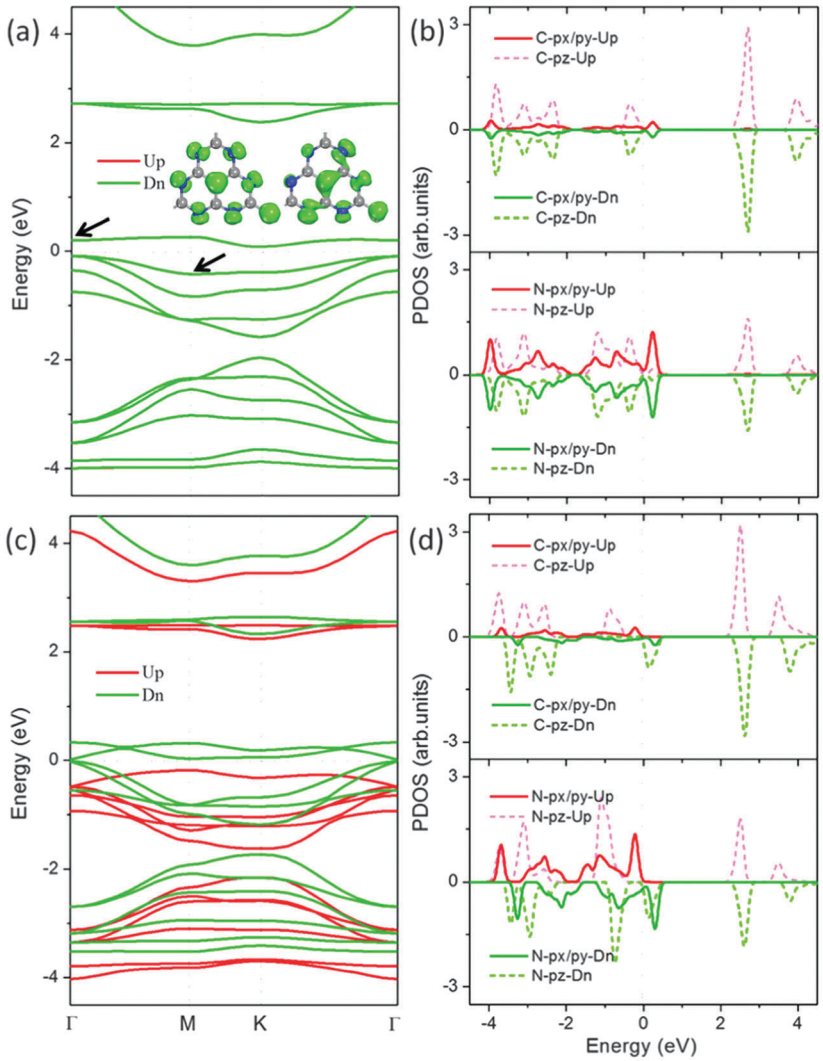

Fig. 4 Band structure (a) and partial DOS (b) for the free g-t-C_4N_3. (c) and (d) for the strained g-t-C_4N_3 with a tensile strain of 4.0%, respectively. The inset figures are the partial charge densities for the conduction and valance bands marked with arrows, respectively.

A sites, and their neighboring sites as B sites. The tri-ring unit can be seen as a zigzag edged triangular nanoflake.[23,24] When a tensile strain is applied, the spin-up p orbitals of both C and N atoms are down-shifted, and the spin-down p_z orbitals are up-shifted. When the tensile strain is increased to 4.0%, the 2D porous sheet becomes a FM semi-metal (the band gap is about 34 meV). The corresponding band structure and PDOS are shown in Fig. 4(c) and (d). There are two spin split energy bands near the Fermi level which are mainly contributed by p_z orbitals of both the A sites (C and N atoms) and p_x and p_y orbitals of the N atoms. The total magnetic moment is 2.0 μ_B per unit cell. In order to reconfirm our results, the HSE06 hybrid functional,[25] which has been proved to be more accurate in predicting the fundamental band gap of solids, is used to calculate the electronic and magnetic properties. We found that the free g-t-C_4N_3 is a NM semiconductor with a band gap of 0.7 eV and the above results of NM–FM transition under tension strain still hold in the hybrid DFT level.

In order to study the magnetic coupling, we calculated the energy difference between the FM and NM/AFM states. For the free g-t-C_4N_3, the NM coupling state is lower in energy by 0.14 eV/(2 × 2 unit cells) than the FM state. However, the FM coupling configuration becomes lower in energy than the NF one, and carries a magnetic moment of 2.0 μ_B per unit cell when applying a tensile strain larger than 3.0%. The total energy difference between the FM and AFM states is calculated to be 0.11, 0.17, 0.16 eV/(2 × 2 unit cells) when applying a tensile strain of 3.0%, 4.0%, and 5.0%, respectively, suggesting that 4% is the optimal tensile strain for inducing ferromagnetism. The strain-induced NM–FM transition can be understood from the changes in the geometric structure and charge re-distribution induced by tensile strain. As discussed above, due to the strong binding within the tri-rings, the applied tensile strain mainly elongates the bonds connected to the *linking site* and weakens the corresponding C–C covalent bonding as shown in Fig. 5(a) and (b). For example, in the free g-t-C_4N_3 sheet, the

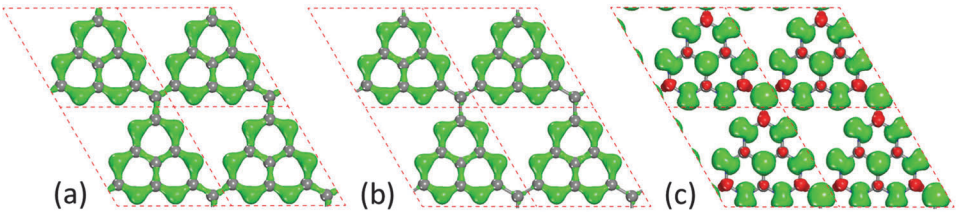

Fig. 5 (a) and (b) 3D charge distribution with 1.8 eÅ^{-3} for the free and strained (4.0%) g-t-C_4N_3. (c) Iso-surfaces of spin density with 0.02 μ_BÅ^{-3} for the g-t-C_4N_3 with a tensile strain of 4.0%. The green and red colors in (c) represent spin up and spin down electrons, respectively.

lengths of C–N and C–C bonds in a tri-ring are d_{C-N} = 1.342–1.353 Å and d_{C-C} = 1.422 Å, respectively. The length of C–C bonds at the linking site is 1.441 Å which is increased to 1.534 Å when applying a tensile strain of 3.0%, while the other bonds are only slightly stretched (d_{C-N} = 1.359–1.362 Å, d_{C-C} = 1.425 Å). The stretched bonds at the linking site significantly enhance the magnetic moment on the linking site (as shown in Fig. 5c), which can effectively mediate the magnetic coupling between the tri-ring units. Accordingly the system can exhibit a stable long-ranged ferromagnetism.

To further understand the impact of strain on the optical properties of the new g-t-C_4N_3 structure, we calculate the dielectric functions for the equilibrium geometry (Fig. 6a) and for structures with tensile strains of 2% and 4% (Fig. 6b and c). In the free state, the new structure has sharp absorption peaks and strong absorption intensity, where the peaks 1 and 2 are in the infrared range (<1.0 eV), which correspond to the optical transition from valence bands to the CBM that is mainly contributed by p_x and p_y orbitals of the N atoms, while the peaks 3 and 4 are in the visible range (2–4 eV) and correspond to the adsorption to the next conduction band contributed by p_z orbitals of the C and N atoms as shown in Fig. 4(a) and (b). The outstanding light absorption capacity of the new g-t-C_4N_3 originates from the fact that its electronic band dispersion near the Fermi level is extremely flat. However, when a strain is applied, the peaks 1, 3 and 4 are down-shifted, while the peak 2 almost remains unchanged. With the tensile strain reaching 4%, due to the energy band splitting, the peak 3 is weakened while the peak 4 is enhanced resulting in a stronger adsorption peak at around 3.3 eV, as shown in Fig. 6(c). From the above discussions we can conclude that the strain can not only induce ferromagnetism but also tune the optical absorption spectrum. Delicate manipulation of the physical properties of this new structure can thus be envisioned.

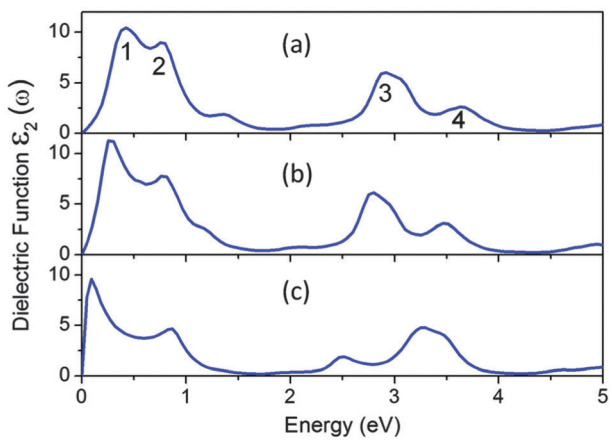

Fig. 6 Imaginary part of dielectric function for parallel polarization in the energy range of 0 to 5 eV for the free (a) and strained g-t-C_4N_3 with a tensile strain of 2% (b) and 4% (c).

In summary, based on first-principles calculations, we predicted a new structure of a g-C_4N_3 sheet consisting of the tri-ring heptazine-like units, namely, the g-t-C_4N_3, which shows some new features as compared to the previously suggested structure, the g-s-C_4N_3, composed of the single-ring triazine units: (1) it is energetically more favorable than the g-s-C_4N_3, and it is also dynamically and thermally stable as confirmed by the phonon spectrum and molecular dynamics calculations; (2) the new structure has sharper optical absorption peaks and stronger absorption intensity; (3) due to the larger pores, the new structure has smaller elastic constants and is more isotropic, which is suitable as a filtration membrane for bigger molecules; (4) although the new structure is nonmagnetic, a small tensile strain can induce a long-ranged ferromagnetism. Our study would provide some new insights for better understanding g-C_4N_3 based 2D porous sheets, and would encourage new experimental efforts in this direction for synthesis and applications.

Acknowledgements

This work is supported by grants from the National Natural Science Foundation of China (grant no. NSFC-11174014 and NSFC-21273012) and the National Grand Fundamental Research 973 Program of China (grant no. 2012CB921404). Xiaowei Li would like to acknowledge the support from China Postdoctoral Science Foundation (grant no. 2012M510246).

Notes and references

1 Y. Wang, X. Wang and M. Antonietti, *Angew. Chem., Int. Ed.*, 2012, **51**, 68.
2 X. Wang, S. Blechert and M. Antonietti, *ACS Catal.*, 2012, **2**, 1596.
3 Y. Zheng, J. Liu, J. Liang, M. Jaroniec and S. Z. Qiao, *Energy Environ. Sci.*, 2012, **5**, 6717.
4 L. Ge, F. Zuo, J. Liu, Q. Ma, C. Wang, D. Sun, L. Bartels and P. Feng, *J. Phys. Chem. C*, 2012, **116**, 13708.
5 S. Min and G. Lu, *J. Phys. Chem. C*, 2012, **116**, 19644.

6 P. Niu, G. Liu and H. Cheng, *J. Phys. Chem. C*, 2012, **116**, 11013.
7 Q. Xiang, J. Yu and M. Jaroniec, *J. Phys. Chem. C*, 2011, **115**, 7355.
8 J. Sehnert, K. Baerwinkel and J. Senker, *J. Phys. Chem. B*, 2007, **111**, 10671.
9 A. Du, S. Sanvito and S. C. Smith, *Phys. Rev. Lett.*, 2012, **108**, 197207.
10 Q. Wang, Q. Sun and P. Jena, *Phys. Rev. Lett.*, 2005, **95**, 167202.
11 J. C. Carrero-Sánchez, A. L. Elías, R. Mancilla, G. Arrellín, H. Terrones, J. P. Laclette and M. Terrones, *Nano Lett.*, 2006, **6**, 1609.
12 X. W. Li, J. Zhou, Q. Wang, Y. Kawazoe and P. Jena, *J. Phys. Chem. Lett.*, 2013, **4**, 259.
13 Y. Xu and S.-P. Gao, *Int. J. Hydrogen Energy*, 2012, **37**, 11072.
14 G. Kresse and J. Furthmuller, *Phys. Rev. B: Condens. Matter Mater. Phys.*, 1996, **54**, 11169.
15 J. P. Perdew, K. Burke and M. Ernzerhof, *Phys. Rev. Lett.*, 1996, **77**, 3865.
16 A. Togo, F. Oba and I. Tanaka, *Phys. Rev. B: Condens. Matter Mater. Phys.*, 2008, **78**, 134106.
17 Y. L. Page and P. Saxe, *Phys. Rev. B: Condens. Matter Mater. Phys.*, 2002, **65**, 104104.
18 X. Wu, D. Vanderbilt and D. R. Hamann, *Phys. Rev. B: Condens. Matter Mater. Phys.*, 2005, **72**, 035105.
19 M. Gajdoš, K. Hummer, G. Kresse, J. Furthmüller and F. Bechstedt, *Phys. Rev. B: Condens. Matter Mater. Phys.*, 2006, **73**, 045112.
20 A. Du, S. Sanvito, Z. Li, D. Wang, Y. Jiao, T. Liao, Y. H. Ng, Z. Zhu, R. Amal and S. C. Smith, *J. Am. Chem. Soc.*, 2012, **134**, 4393.
21 C. Lee, X. Wei, J. W. Kysar and J. Hone, *Science*, 2008, **321**, 385.
22 F. Liu, P. Ming and J. Li, *Phys. Rev. B: Condens. Matter Mater. Phys.*, 2007, **76**, 064120.
23 S. H. Zhang, J. Zhou, X. W. Li and Q. Wang, *J. Nanopart. Res.*, 2012, **14**, 1171.
24 J. Zhou, Q. Wang, Q. Sun and P. Jena, *Phys. Rev. B: Condens. Matter Mater. Phys.*, 2011, **84**, 081402(R).
25 J. Heyd, G. E. Scuseria and M. Ernzerhof, *J. Chem. Phys.*, 2006, **124**, 219906.

